



**HAL**  
open science

## **In situ monitoring of electric field effect on domain wall motion in Co ultrathin films in direct contact with an electrolyte**

A. Lamirand, J.-P. Adam, D. Ravelosona, P. Allongue, F. Maroun

► **To cite this version:**

A. Lamirand, J.-P. Adam, D. Ravelosona, P. Allongue, F. Maroun. In situ monitoring of electric field effect on domain wall motion in Co ultrathin films in direct contact with an electrolyte. *Applied Physics Letters*, 2019, 115 (3), pp.032402. <10.1063/1.5109024>. <hal-02324681>

**HAL Id: hal-02324681**

**<https://hal.science/hal-02324681v1>**

Submitted on 22 Oct 2019


**HAL** is a multi-disciplinary open access archive for the deposit and dissemination of scientific research documents, whether they are published or not. The documents may come from teaching and research institutions in France or abroad, or from public or private research centers.

L'archive ouverte pluridisciplinaire **HAL**, est destinée au dépôt et à la diffusion de documents scientifiques de niveau recherche, publiés ou non, émanant des établissements d'enseignement et de recherche français ou étrangers, des laboratoires publics ou privés.



HAL Authorization

## AUTHOR QUERY FORM








	<p><b>Journal:</b> Appl. Phys. Lett.</p> <p><b>Article Number:</b> 002928APL</p>	<p>Please provide your responses and any corrections by annotating this PDF and uploading it to AIP's eProof website as detailed in the Welcome email.</p>
---	---	--

Dear Author,

Below are the queries associated with your article; please answer all of these queries before sending the proof back to AIP.

**Article checklist:** In order to ensure greater accuracy, please check the following and make all necessary corrections before returning your proof.

1. Is the title of your article accurate and spelled correctly?
2. Please check affiliations including spelling, completeness, and correct linking to authors.
3. Did you remember to include acknowledgment of funding, if required, and is it accurate?

Location in article	Query / Remark: click on the Q link to navigate to the appropriate spot in the proof. There, insert your comments as a PDF annotation.
<p>AQ1 </p> <p>AQ2 </p>	<p>Please check that the author names are in the proper order and spelled correctly. Also, please ensure that each author's given and surnames have been correctly identified (given names are highlighted in red and surnames appear in blue).</p> <p>Please provide issue number for Ref. 21.</p> <p>Please confirm ORCID's are accurate. If you wish to add an ORCID for any author that does not have one, you may do so now. For more information on ORCID, see <a href="https://orcid.org/">https://orcid.org/</a>.</p> <p>A. D. Lamirand - 0000-0003-3016-1377</p> <p>J.-P. Adam </p> <p>D. Ravelosona </p> <p>P. Allongue </p> <p>F. Maroun </p> <hr/> <p>Please check and confirm the Funder(s) and Grant Reference Number(s) provided with your submission:</p> <p>Agence Nationale de la Recherche, Award/Contract Number 16-CE24-0018-04 </p> <p>Please add any additional funding sources not stated above:</p>

Thank you for your assistance.

# *In situ* monitoring of electric field effect on domain wall motion in Co ultrathin films in direct contact with an electrolyte

Cite as: Appl. Phys. Lett. **115**, 000000 (2019); doi: [10.1063/1.5109024](https://doi.org/10.1063/1.5109024)

Submitted: 5 May 2019 · Accepted: 23 June 2019 ·

Published Online: 0 Month 0000



View Online



Export Citation



CrossMark

A. D. Lamirand,<sup>1,2</sup>  J.-P. Adam,<sup>2</sup> D. Ravelosona,<sup>2</sup> P. Allongue,<sup>1</sup> and F. Maroun<sup>1,a)</sup>

## AFFILIATIONS

<sup>1</sup>Physique de la Matière Condensée, Ecole Polytechnique, CNRS, IP Paris, 91128 Palaiseau, France

<sup>2</sup>C2N – CNRS, Université Paris-Sud, Université Paris-Saclay, 91120 Palaiseau, France

<sup>a)</sup> Author to whom correspondence should be addressed: [fouad.maroun@polytechnique.edu](mailto:fouad.maroun@polytechnique.edu)

## ABSTRACT

We present experimental data on the electric field effect on the magnetic domain wall dynamics in Co ultrathin films in direct contact with an aqueous electrolyte and in the absence of any oxide layer. We use a three electrode electrochemical setup to apply a large and uniform electric field and to precisely separate chemical effects induced by hydrogen from pure electric field effects. We show that in the case of the pure electric field effect, the domain wall velocity varies exponentially with the electric field and that these variations are larger than those observed previously on similar systems due to a large magnetoelectric coefficient in our case.

Published under license by AIP Publishing. <https://doi.org/10.1063/1.5109024>

Domain wall (DW) motion in perpendicularly magnetized ferromagnets is a field of intensive research.<sup>1–3</sup> DWs may be displaced by applying an external magnetic field<sup>4</sup> or by injecting an electric current.<sup>5–7</sup> In spite of the large current densities required and the associated heat generation and power consumption, the latter process is of the greatest technological relevance since it allows controlling the motion of a larger number of neighboring DWs in racetrack memories<sup>3</sup> and addressing individual magnetic nanodevices as memristors.<sup>8</sup> An elegant approach to reduce the current density and the device power consumption is to lower the magnetic anisotropy energy (MAE) that controls the DW depinning and the motion process. A promising means to achieve this goal is to apply a voltage across an insulating layer between a gate electrode and the ferromagnetic layer to modify the layer MAE.<sup>9</sup> This method, usually called voltage control of magnetization (VCM), has been widely investigated experimentally and theoretically<sup>9–11</sup> since the early publication of Weisheit *et al.*<sup>12</sup> More recent studies have demonstrated that magnetic DW velocity in ultrathin films can be modified by the application of a voltage.<sup>4,13–17</sup>

When considering metallic ferromagnets in contact with an insulating layer, VCM is related to several effects. The first effect is the potential induced accumulation of charges at the ferromagnet surface,<sup>12,18</sup> which is commonly called the electric field effect (EFE). The second effect is related to the modification of the ferromagnet surface chemistry either by oxidation at the ferromagnet/oxide interface<sup>19</sup> or at the solid/electrolyte contact<sup>20</sup> or by molecular adsorption at the

ferromagnet surface in electrolytes.<sup>18</sup> This effect is usually called the magnetoionic effect. The latter process induces large MAE modification reaching several  $100 \text{ fJ V}^{-1} \text{ m}^{-1}$ , while MAE induced by charge accumulation is generally small (a few  $10 \text{ fJ V}^{-1} \text{ m}^{-1}$ ).<sup>9</sup>

The large majority of the experimental studies has been performed on solid state devices using an insulating layer which may induce chemical modification of the magnetic layer in the presence of an external electric field. Gating directly through an electrolyte, i.e., putting the ferromagnetic layer in direct contact with an electrolyte, is appealing as it prevents possible artifacts induced by the insulating layer and allows the application of larger electric fields.<sup>12</sup> However, the major drawback of this approach is the sample oxidation during its transfer in air between the sample preparation chamber and the cell where magnetic measurements are performed. One alternative approach used by us and others combines *in situ* electrodeposition and magnetic characterization in a single electrochemical cell which avoids transfer of the sample through air.<sup>18,20–23</sup>

In this work, we investigate the voltage control of MAE and the DW velocity in Co layers in direct contact with an electrolyte and in the absence of any insulating layer using *in situ* magneto-optical Kerr effect (MOKE) imaging of magnetic domains and complementary *in situ* MOKE characterization. We used a specific experimental procedure for contacting Co ultrathin epitaxial layers with an electrolyte *in situ* avoiding any transfer in air and surface oxide formation. In this procedure which was successfully used in recent studies,<sup>18,21</sup> an

70 ultrathin epitaxial Co layer is grown *in situ* by electrodeposition in the  
71 cell used for MOKE measurements. Using this approach, we clearly  
72 separate EFE from the magnetoionic effect in an electric field range  
73 comparable to that in solid state device studies. We also show that in  
74 the case of EFE, the DW velocity varies exponentially with the electric  
75 field but with a larger variation coefficient.

76 The Co films ( $\sim 0.8$  nm thick) were electrodeposited on a Pd/Au/  
77 Si(111) substrate *in situ* in a custom three electrode electrochemical  
78 flow cell,<sup>18,24,25</sup> which was inserted either in the MOKE setup or in the  
79 MOKE microscope and connected to a potentiostat. The sample structure  
80 and the cell are sketched in the [supplementary material](#) (Fig. S1).  
81 The atomically flat Au(111) buffer layers (8 nm thick) were prepared  
82 by epitaxial electrodeposition on Si(111).<sup>26</sup> The Co layers were covered  
83 by a monolayer of carbon monoxide to increase the layer out-of-plane  
84 anisotropy and to widen the Co film potential stability range.<sup>18</sup> All  
85 magnetic characterization presented below is conducted under a con-  
86 tinuous flow of 0.1 M  $K_2SO_4$  + 1 mM  $H_2SO_4$  + 1 mM KCl saturated  
87 with CO. MOKE results on CO covered Co layers deposited on  
88 Au/Si(111) samples without a Pd underlayer are given in the [supple-](#)  
89 [mentary material](#) for comparison. The polar MOKE setups are home-  
90 built and described in previous works and in the [supplementary](#)  
91 [material](#).<sup>18,20,21</sup> The cell is installed vertically between the two poles of  
92 an electromagnet, which applies a magnetic field perpendicular to the  
93 sample surface. DW velocity  $v$  was determined from the traveling dis-  
94 tance of the DW during the propagation magnetic pulse averaged over  
95 the entire domain.

96 The CO covered Co/Pd/Au/Si(111) samples in contact with the  
97 electrolyte are perpendicularly magnetized as demonstrated by square  
98  $M$ - $H$  curves with a high coercive field ( $H_C$ ) measured at different  
99 potentials in the range of  $-0.8$  V to  $-1.3$  V [see insets of Fig. 1(a)].  
100 The variation of  $H_C$  during a potential sweep from  $-0.8$  V to  $-1.3$  V  
101 and backward is presented in Fig. 1(a) (open symbols) together with  
102 the electrochemical current (solid line). One notices two distinct  
103 regimes: for potentials  $U > -1$  V,  $H_C$  varies quasilinearly with a nega-  
104 tive slope, and for  $U < -1$  V,  $H_C$  decreases, while a significant electro-  
105 chemical current starts to flow. This decrease is concomitant with the  
106 onset of the electrochemical reaction where  $H^+$  cations in the electro-  
107 lyte are transformed into  $H_2$  gas through the hydrogen evolution reac-  
108 tion (HER)  $2H^+ + 2e^- \rightarrow H_2$ .<sup>27</sup> Since the observed  $H_C$  behavior in  
109 the HER regime is quasiabsent in the absence of the Pd underlayer  
110 (see the [supplementary material](#), Fig. S3), the prominent decrease in  
111  $H_C$  below  $-1$  V observed in Fig. 1(a) suggests that the effect related to  
112 HER is specific to the presence of the Pd underlayer.

113 In Fig. 1(b), we present the ratio  $\Delta H_C/H_C^0$ , the relative variation  
114 of  $H_C$  with respect to  $H_C^0$ , the value of  $H_C$  for  $U = -0.8$  V.  $\Delta H_C/H_C^0$   
115 is plotted as a function of potential measured at different time delays  $t$   
116 after the potential step [see the inset in Fig. 1(b)]. The  $\Delta H_C/H_C^0$  time  
117 transient is composed of an instantaneous jump followed by a slow  
118 decay with a time constant  $\tau$ , before a steady state value is reached (see  
119 also Fig. S2). If measured at  $t > \tau$  after a potential step (red open sym-  
120 bols and red line are guides to the eye),  $\Delta H_C/H_C^0$  follows a trend simi-  
121 lar to that measured during a potential sweep [Fig. 1(b) black curve],  
122 with a maximum around  $-1.05$  V. The results change considerably  
123 when considering the values of  $\Delta H_C/H_C^0$  acquired immediately after  
124 the potential jump [Fig. 1(b) black stars and black line are guides to  
125 the eye]. In this case, the variation is almost linear with time over the  
126 entire potential range. By comparison,  $\Delta H_C/H_C^0$  is a linear and

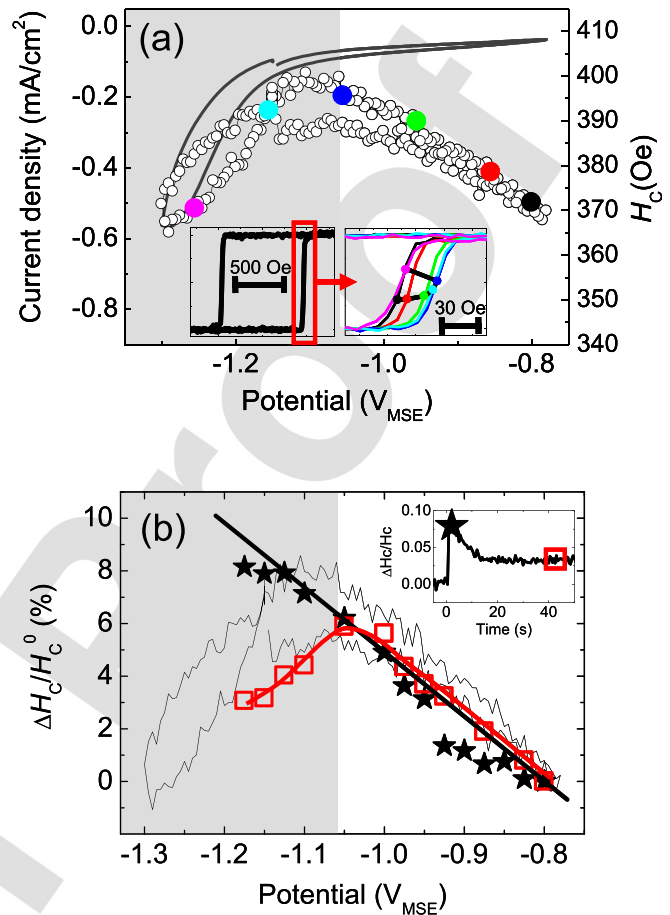
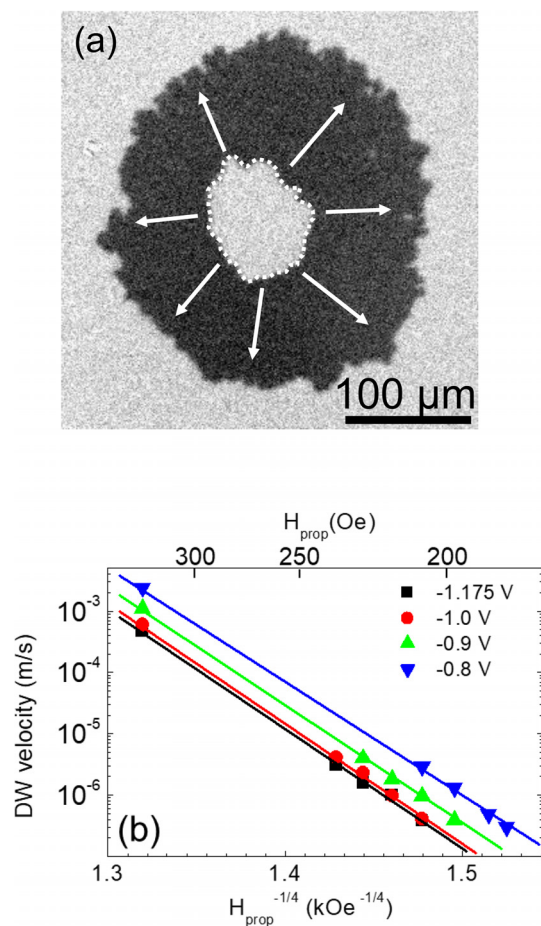


FIG. 1. (a) Potential induced variations of coercive field  $H_C$  and electrochemical current upon sweeping the potential at a rate of 20 mV/s. Insets: left, normalized  $M$ - $H$  curve of the sample and right, a selection of  $M$ - $H$  curves during a potential sweep with a zoom on one edge of the  $M$ - $H$  curve. The different colors correspond to various potentials between  $-0.8$  V and  $-1.3$  V. (b) Potential dependence of  $\Delta H_C/H_C^0$  measured in steady state conditions (red open squares) or immediately after the application of the potential step (black stars). The black curve corresponds to the potential sweep experiment shown in (a). The black and red lines are guides to the eye. The inset shows  $\Delta H_C/H_C^0$  as a function of time during a potential step. The black star and the red square indicate which values are used in the main plots.

reversible function of the applied potential over the same potential  
range for CO-covered Co/Au/Si(111) samples in both potential step  
and potential sweep experiments (see Fig. S3). Consequently, the effect  
induced by the HER may be completely avoided by shortening the resi-  
dence time, i.e., the time spent by the sample in this potential range.

We now focus on voltage control of DW velocity ( $v$ ). Figure 2(a)  
presents a typical image of the magnetic domain in Co/Pd/Au/Si(111)  
films obtained by polar MOKE microscopy, by subtracting two images  
taken after applying the  $H_{nuc}$  nucleation pulse and  $H_{prop}$  propagation  
pulse. The magnetic domain propagates within the dark crown from the  
center to the edge (see white arrows). The circular shape of the crown  
suggests that the DW propagates isotropically, indicating a rather  
homogeneous MAE landscape. The dependence of  $v$  as a function of  
the propagation field  $H_{prop}$  is shown in Fig. 2(b). These measurements



**FIG. 2.** (a) Example of a “differential” MOKE image of a Co(0.8 nm)/Pd/Au/Si(111) sample after the application of a magnetic field pulse (nucleation 220 Oe during 5 ms, propagation 160 Oe during 2 s) at  $U = -0.85$  V to expand an initially formed inverted magnetic domain. (b) Plots of DW velocity as a function of  $H_{\text{prop}}^{-1/4}$  (in  $\text{kOe}^{-1/4}$ ) measured at different potentials. For clarity, the top x-axis displays the values of  $H_{\text{prop}}$  in Oe.

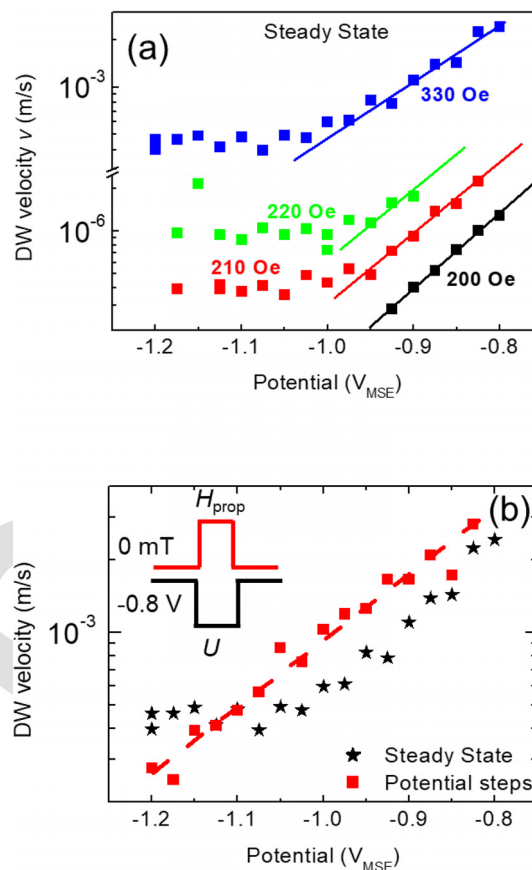


**FIG. 3.** (a) DW velocity as a function of the potential at different magnetic fields in steady state conditions (where the potential is constant during the entire MOKE image acquisition). A break is introduced along the y-axis to compensate for the rapid increase in  $v$  with  $H_{\text{prop}}$  between 220 and 330 Oe. (b) DW velocity as a function of the potential pulse amplitude at 330 Oe. In this case, all images are recorded at a potential of  $-0.8$  V and the pulses of the field and potential are synchronized as shown in the drawing in the inset. Note the exponential law (red line).

are performed in conditions where the potential is constant during the entire MOKE image acquisition (few seconds). This procedure will be called hereafter steady state conditions. The linear dependence of the logarithm of  $v$  as a function of  $H_{\text{prop}}^{-1/4}$  indicates that the DW propagation is in the creep regime, i.e., the propagation of the wall is dominated by thermal activation over the energy barrier of pinning sites, and follows the phenomenological equation,<sup>4</sup>

$$v = v_0 \exp\left[-(U_C/kT)(H_{\text{prop}}/H_{\text{dep}})^{-1/4}\right]. \quad (1)$$

In this equation,  $v_0$  is a numerical prefactor,  $T$  is the temperature,  $k$  is the Boltzmann factor,  $H_{\text{dep}}$  is the depinning magnetic field, and  $U_C$  is the disorder-induced energy barrier arising from the collective pinning of small DW sections. Figure 3(a) presents the dependence of  $v$  (on a logarithmic scale) as a function of potential for different values of  $H_{\text{prop}}$ . For  $U > -1$  V, the plots are linear with a slope quasi-independent of  $H_{\text{prop}}$ . Conversely, for  $U < -1$  V, the DW velocity

becomes quasi-independent of the potential, a phenomenon which is concomitant with the regime change of  $H_C$  variations observed in Fig. 1(b). These results suggest that  $H_C$  and  $v$  variations as a function of potential are due to the potential dependence of the Co layer MAE. In order to study  $v$  without the influence of the HER, we performed experiments where the residence time at a potential  $U$  is short and all MOKE images are acquired at a rest potential of  $-0.8$  V, i.e., outside the HER region. For these experiments, potential and magnetic field pulses are synchronized and last typically 0.2 s. Figure 3(b) presents data measured using this procedure (red squares) together with the steady state measurements (black stars) for a magnetic field of 330 Oe. One clearly observes that using this second procedure  $v$  follows an exponential dependence over the full potential range. The slope is slightly different from the one measured in steady state conditions (for  $U > -1$  V), and the two plots are slightly shifted. The origin of these differences may probably be a reorganization of the Co surface in contact with the electrolyte, after long steady state measurements over several hours.

The polar MOKE and polar MOKE microscopy results clearly show that the more positive the electrochemical potential, the larger the DW velocity and the lower the coercive field. In agreement with our previous studies,<sup>18</sup> this is consistent with a decrease in the MAE at more negative potentials induced by the electric field at the electrolyte/Co interface. In addition to this trend, three main outcomes of this work can be highlighted: (i) *in situ* grown Co layers in contact with an electrolyte present large propagating magnetic domains which can be observed by *in situ* MOKE microscopy, and their DW propagation velocity  $v$  follows the creep regime equation in the explored magnetic field range; (ii)  $v$  could be measured at high electric fields (up to 3 V/nm) in the absence of an intermediate oxide layer and in the absence of any chemical effect; (iii)  $v$  varies exponentially with the applied potential in the absence of chemical effect and becomes quasi-independent of the potential in the HER range. These variations are entirely reversible and take place with a short time constant, corresponding to the one of the electrochemical cell we used in this study (20 ms).

The first outcome suggests that these electrochemically grown Co films in direct contact with the electrolyte present a low and homogeneous density of defects as shown in previous *in situ* scanning tunneling microscopy and *in situ* X ray diffraction studies of the Co layer grown on Au(111).<sup>28,29</sup> These flat Co layers yield a DW propagation regime similar to what is observed in solid state devices prepared by sputtering deposition. It is interesting to note that we obtain  $v$  values similar to those for solid state samples with a similar Co thickness and at a  $H_{prop}$  value of 250 Oe as AlOx/Co/Pt<sup>13</sup> and HfO<sub>2</sub>/MgO/Co/Pt (after extrapolation to higher magnetic fields).<sup>17</sup>

The second outcome is directly related to our approach: (i) we grow the ferromagnetic layer *in situ* in an electrochemical environment with the potential control over the sample ensuring that no Co oxide is formed and (ii) the direct contact of the Co layer with the electrolyte allows applying large electric fields which are spatially homogeneous using low applied voltages. This ferromagnetic metal/electrolyte contact with potential control ensures the separation of the pure charge accumulation effect from other effects. In solid state devices, the dielectric layer often interferes in the EFE signal because of electric field induced ion migration and charge trapping in the dielectric layer and surface oxidation of the ferromagnetic layer, leading to slow and often irreversible modifications of the MAE. In our case, potential induced chemical modification of the sample which takes place in the HER regime is well characterized and can be avoided if the potential is applied during short periods.

Regarding the last outcome, the exponential dependence of DW velocity  $v$  and the linear variations of  $\Delta H_C/H_C$  with applied potential are consistent with a linear MAE potential dependence and a pure charge accumulation effect at the electrolyte/Co interface. Indeed, in our previous papers,<sup>18,21</sup> we demonstrated that the linear behavior of  $\Delta H_C/H_C$  is related to a linear change of the electrolyte/Co interface MAE  $K_S^{Electrolyte/Co}$ . We also showed that whenever electrochemical effects are involved, nonlinear variations of  $\Delta H_C/H_C$  are observed as a function of potential.<sup>18</sup> The exponential dependence of  $v$  with applied potential linked to a linear modification of the interface anisotropy energy is also consistent with the interpretation given in Ref. 13.

We now compare the potential dependence of the velocity for electrolyte/Co/Pd/Au/Si(111) with other studies on solid state devices. In the study of Ref. 13, the influence of the potential on  $v$  was

measured at 220 Oe (as in our study), and the range of  $v$  as a function of the propagation field is very similar to that measured in our study. This suggests that the parameters in the expression of  $v$  are also similar in both cases. To compare quantitatively the potential dependence of  $v$ , we rewrite the expression governing  $v$  in the creep regime,

$$v(E) = v_0 \exp \left[ -\alpha(E)(H_{prop})^{-1/4} \right], \quad (2)$$

where  $E$  is the electric field and  $\alpha = (U_C/kT)(H_{dep})^{1/4}$ . Following the derivation done in Ref. 13,  $\alpha$  is proportional to the MAE,

$$\alpha(E) = \alpha_0 \left[ K_V + \left( K_S^{Total} + \beta E \right) / d \right], \quad (3)$$

where  $\alpha_0$  contains different micromagnetic parameters of the magnetic layer,  $K_V$  is the Co bulk MAE,  $K_S^{Total} = K_S^{Co/Pd} + K_S^{Electrolyte/Co}$ , with  $K_S^{Co/Pd}$  being the Co/Pd interface MAE and  $K_S^{Electrolyte/Co}$  the electrolyte/Co interface MAE,  $d$  is the layer thickness, and  $\beta$  is the EFE coefficient, i.e., the variation coefficient per  $V m^{-1}$  of  $K_S^{Electrolyte/Co}$ . We assumed that  $K_S^{Electrolyte/Co}$  is linear with the electric field. It is convenient to estimate the electric field difference  $\Delta E = E_1 - E_2$  necessary to increase  $v$  by one order of magnitude, the smaller the  $\Delta E$ , the larger the EFE. Using Eqs. (2) and (3), we can write

$$v(E_1)/v(E_2) = \exp \left[ -\alpha_0(\beta/d)(H_{prop})^{-1/4} \Delta E \right] = 10. \quad (4)$$

The fit of the data in Fig. 2(b) does not allow obtaining a consistent trend in the potential dependence of the parameters governing  $v$ . This is due to the large uncertainty on the fitted slope and offset most probably because of the small range of available magnetic field. It is therefore more accurate to use the potential dependence of  $v$  measured at a fixed magnetic field. From the fit of the data in the exponential regime in Fig. 3(a) and considering that the distance between the charged planes responsible for the EFE is  $\sim 0.14$  nm (see Fig. S1),<sup>21</sup> we obtain  $\Delta E \sim 1.5$  V/nm. In the case of AlOx/Co/Pt, the AlOx thickness is 3.8 nm and the data reported in Ref. 13 yield  $\Delta E \sim 4$  V/nm. Consequently, the EFE is 2.7 times larger in our case as compared to Ref. 13. This is related to one of the parameters inside the exponential term. The cobalt thickness  $d$  and  $H_{prop}$  are similar in both studies. The parameter  $\alpha_0$  should be also similar for both systems since the measured DW velocity is similar for similar  $H_{prop}$ . Consequently, the difference should come from the  $\beta$  coefficient. In our case,  $\beta$  equals  $34 \text{ fJ V}^{-1} \text{ m}^{-1}$ ,<sup>18</sup> whereas it amounts to  $14 \text{ fJ V}^{-1} \text{ m}^{-1}$  for AlOx/Co/Pt,<sup>13</sup> i.e., 2.4 times smaller, a value very close to that obtained above, 2.7. This indicates that the higher EFE measured in our case is essentially due to the higher value of the parameter  $\beta$  in our work. The difference between the two systems may originate from the orbital shape of the Co atoms which are bonded to the carbon atoms of the CO overlayers in our case and to oxygen in the case of the AlOx/Co interface. The comparison with HfO<sub>2</sub>/MgO/Co/Pt is less straightforward because  $v$  at 220 Oe is two orders of magnitude larger than in our case.<sup>17</sup> In addition, the value of  $\beta$  in this study is very large ( $\sim 150 \text{ fJ V}^{-1} \text{ m}^{-1}$ ), well above the range of  $10\text{--}50 \text{ fJ V}^{-1} \text{ m}^{-1}$  of  $\beta$  values usually measured for Co and CoFeB layers,<sup>30–34</sup> which suggests that chemical processes might be involved.

In steady-state conditions and in the HER region, i.e., at potentials between  $-1$  V and  $-1.3$  V, the DW velocity levels off and deviates from the exponential law, suggesting the presence of a second effect on

MAE with the opposite sign compensating the EFE. In the CO saturated electrolyte, this second regime exists only in the presence of the Pd underlayer and is concomitant with significant changes of the sample reflectivity (see Fig. S4). Since it was previously observed that Pd reflectivity changes upon H-insertion/release,<sup>35</sup> we infer that this second effect on MAE is connected with the insertion and removal of atomic hydrogen in and out of the Pd layer. Magnetic studies of Co/Au(111) layers capped with Pd clearly show that H loading into Pd modifies the Co MAE.<sup>35</sup> A similar phenomenon can be expected in our case, provided that the H can reach the Pd underlayer, either by diffusion through the Co layer or directly in the Pd layer through pinholes in the Co layer.

The magnetic domains of electrodeposited perpendicularly magnetized Co epitaxial layers were imaged by MOKE microscopy, while the sample surface is oxide-free and in contact with an electrolyte. The domain walls propagate in the creep regime, and the velocity varies exponentially with the potential (slope  $\sim 2.5$  decades/V). The exponential variation originates from the linear variations of the surface anisotropy energy with potential (i.e., charge accumulation at the surface), and a quantitative comparison with literature suggests that the slope scales with the parameter  $\beta$  used to characterize the efficiency of the electric field effect on MAE, which is  $\sim 2.5$  larger at the electrolyte/Co than at the AlOx/Co interface. In the steady state condition and at potential where HER settles in, the DW velocity levels off, probably due to hydrogen incorporating in the Pd underlayer.

See the [supplementary material](#) for complete experimental details and additional magnetic and reflectivity results of Co/Pd/Au/Si(111) and Co/Au/Si(111) samples.

This work was supported by two public grants from the French National Research Agency (ANR): Labex NanoSaclay, reference: ANR-10-LABX-0035, and ELECSPIN ANR-16-CE24-0018-04.

### 313 REFERENCES

- 314 <sup>1</sup>C. Chappert, A. Fert, and F. N. Van Dau, *Nat. Mater.* **6**(11), 813–823 (2007).
- 315 <sup>2</sup>D. A. Allwood, G. Xiong, C. C. Faulkner, D. Atkinson, D. Petit, and R. P. Cowburn, *Science* **309**(5741), 1688–1692 (2005).
- 316 <sup>3</sup>S. S. P. Parkin, M. Hayashi, and L. Thomas, *Science* **320**(5873), 190–194 (2008).
- 317 <sup>4</sup>P. J. Metaxas, J. P. Jamet, A. Mougou, M. Cormier, J. Ferré, V. Baltz, B. Rodmacq, B. Dieny, and R. L. Stamps, *Phys. Rev. Lett.* **99**(21), 217208 (2007).
- 318 <sup>5</sup>M. Tsoi, R. E. Fontana, and S. S. P. Parkin, *Appl. Phys. Lett.* **83**(13), 2617–2619 (2003).
- 319 <sup>6</sup>D. Ravelosona, S. Mangin, J. A. Katine, E. F. Eric, and B. D. Terris, *Appl. Phys. Lett.* **90**(7), 072508 (2007).
- 320 <sup>7</sup>C. Burrowes, A. P. Mihai, D. Ravelosona, J. V. Kim, C. Chappert, L. Vila, A. Marty, Y. Samson, F. Garcia-Sanchez, L. D. Buda-Prejbeanu, I. Tudosa, E. E. Fullerton, and J. P. Attane, *Nat. Phys.* **6**(1), 17–21 (2010).
- 321 <sup>8</sup>S. Lequeux, J. Sampaio, V. Cros, K. Yakushiji, A. Fukushima, R. Matsumoto, H. Kubota, S. Yuasa, and J. Grollier, *Sci. Rep.* **6**, 31510 (2016).
- 322 <sup>9</sup>B. Dieny and M. Chshiev, *Rev. Mod. Phys.* **89**(2), 025008 (2017).
- 323 <sup>10</sup>D. Chun-Gang, P. V. Julian, R. F. Sabirianov, Z. Ziqiang, C. Junhao, S. S. Jaswal, and E. Y. Tsybal, *Phys. Rev. Lett.* **101**(13), 137201 (2008).
- 324 <sup>11</sup>K. Nakamura, R. Shimabukuro, T. Akiyama, T. Ito, and A. J. Freeman, *Phys. Rev. B* **80**(17), 172402 (2009).
- 325 <sup>12</sup>M. Weisheit, S. Fahler, A. Marty, Y. Souche, C. Poinsignon, and D. Givord, *Science* **315**(5810), 349–351 (2007).
- 326 <sup>13</sup>A. J. Schellekens, A. van den Brink, J. H. Franken, H. J. M. Swagten, and B. Koopmans, *Nat. Commun.* **3**, 847 (2012).
- 327 <sup>14</sup>A. Bernard-Mantel, L. Herrera-Diez, L. Ranno, S. Pizzini, J. Vogel, D. Givord, S. Auffret, O. Boule, I. M. Miron, and G. Gaudin, *Appl. Phys. Lett.* **102**(12), 122406 (2013).
- 328 <sup>15</sup>U. Bauer, S. Emori, and G. S. D. Beach, *Appl. Phys. Lett.* **100**(19), 192408–192404 (2012).
- 329 <sup>16</sup>H. Kakizakai, K. Yamada, M. Kawaguchi, K. Shimamura, S. Fukami, N. Ishiwata, D. Chiba, and T. Ono, *Jpn. J. Appl. Phys., Part 1* **52**, 070206 (2013).
- 330 <sup>17</sup>D. Chiba, M. Kawaguchi, S. Fukami, N. Ishiwata, K. Shimamura, K. Kobayashi, and T. Ono, *Nat. Commun.* **3**, 888 (2012).
- 331 <sup>18</sup>N. Tournerie, A. P. Engelhardt, F. Maroun, and P. Allongue, *Phys. Rev. B* **86**(10), 104434 (2012).
- 332 <sup>19</sup>F. Bonell, Y. T. Takahashi, D. D. Lam, S. Yoshida, Y. Shiota, S. Miwa, T. Nakamura, and Y. Suzuki, *Appl. Phys. Lett.* **102**(15), 152401 (2013).
- 333 <sup>20</sup>N. Di, J. Kubal, Z. Zeng, J. Greeley, F. Maroun, and P. Allongue, *Appl. Phys. Lett.* **106**(12), 122405 (2015).
- 334 <sup>21</sup>N. Tournerie, A. Engelhardt, F. Maroun, and P. Allongue, *Surf. Sci.* **631**, 88–95 (2015).
- 335 <sup>22</sup>K. Leistner, N. Lange, J. Hänisch, S. Oswald, F. Scheiba, S. Fähler, H. Schlörb, and L. Schultz, *Electrochim. Acta* **81**(Suppl. C), 330–337 (2012).
- 336 <sup>23</sup>K. Duschek, M. Uhlemann, H. Schlörb, K. Nielsch, and K. Leistner, *Electrochim. Commun.* **72**(Suppl. C), 153–156 (2016).
- 337 <sup>24</sup>P. Allongue, F. Maroun, H. F. Jurca, N. Tournerie, G. Savidand, and R. Cortes, *Surf. Sci.* **603**, 1831–1840 (2009).
- 338 <sup>25</sup>P. Allongue and F. Maroun, *MRS Bull.* **35**(10), 761–770 (2010).
- 339 <sup>26</sup>P. Prod'homme, F. Maroun, R. Cortes, and P. Allongue, *Appl. Phys. Lett.* **93**(17), 171901 (2008).
- 340 <sup>27</sup>J. O. M. Bockris and A. K. N. Reddy, *Modern Electrochemistry* (Plenum Press, New York, 1977), Vol. 2.
- 341 <sup>28</sup>C. A. Lucas, F. Maroun, N. Sisson, P. Thompson, Y. Gründer, R. Cortès, and P. Allongue, *J. Phys. Chem. C* **120**(6), 3360–3370 (2016).
- 342 <sup>29</sup>N. Di, A. Damian, F. Maroun, and P. Allongue, *J. Electrochem. Soc.* **163**(12), D3062–D3068 (2016).
- 343 <sup>30</sup>W.-G. Wang, M. Li, S. Hageman, and C. L. Chien, *Nat. Mater.* **11**, 64 (2012).
- 344 <sup>31</sup>S. Kanai, M. Yamanouchi, S. Ikeda, Y. Nakatani, F. Matsukura, and H. Ohno, *Appl. Phys. Lett.* **101**(12), 122403 (2012).
- 345 <sup>32</sup>M. Endo, S. Kanai, S. Ikeda, F. Matsukura, and H. Ohno, *Appl. Phys. Lett.* **96**(21), 212503 (2010).
- 346 <sup>33</sup>U. Bauer, S. Emori, and G. S. D. Beach, *Appl. Phys. Lett.* **101**(17), 172403–172404 (2012).
- 347 <sup>34</sup>W. W. Lin, N. Vernier, G. Agnus, K. Garcia, B. Ocker, W. S. Zhao, E. E. Fullerton, and D. Ravelosona, *Nat. Commun.* **7**, 13532 (2016).
- 348 <sup>35</sup>F. Maroun, F. Reikowski, N. Di, T. Wiegmann, J. Stettner, O. M. Magnussen, and P. Allongue, *J. Electroanal. Chem.* **819**, 322–330 (2018).

AQ2